Applied Science and Engineering Progress, Vol. 20, No. 2, 2027, 8192

Influence of Novel Hydrofluoric Acid and Nitric Acid Etchants on Performance of Photochemical Machining of Ti-6Al-4V Alloy for Biomedical Applications

Pallab Sarmah and Kapil Gupta*
Department of Mechanical and Industrial Engineering Technology, Faculty of Engineering & the Built Environment, University of Johannesburg, Doornfontein Campus, Johannesburg-2028, South Africa

Promod Kumar Patowari
Department of Mechanical Engineering, National Institute of Technology Silchar, Silchar-788010, India

* Corresponding author. E-mail: kgupta@uj.ac.za DOI: 10.14416/j.asep.2026.04.008
Received: 16 February 2026; Revised: 17 March 2026; Accepted: 17 April 2026; Published online: 24 April 2026

Abstract
Photochemical machining (PCM) process is widely recognized for the fabrication of precision engineering parts and components. This study examines the impact of novel hybrid Hydrofluoric Acid (HF) and Nitric Acid (HNO_3) etchant compositions on the PCM performance for cutting square-shaped (5 mm × 5 mm) cavities in Ti-6Al-4V alloy for biomedical component manufacturing. A total of 25 experiments were performed to determine the effects of etching composition and time on edge deviation (ED), material removal rate (MRR), and mean roughness depth (Rz). The novel HF-HNO_3 etchant enables precise PCM machining of Ti-6Al-4V, achieving minimum ED (29 µm) and Rz (1.82 µm) and maximum MRR (0.967 mg/min). The HF-HNO_3 composition was found to significantly affect etching kinetics, thereby affecting process productivity and the integrity of the machined surface. The findings provide deep insight into the etching behaviour of Ti-6Al-4V and establish process directions for applying PCM in the manufacturing of biomedical components.

Keywords: Biomedical application, Edge deviation, HF-HNO_3, Photochemical machining, Surface roughness, Ti-6Al-4V

1 Introduction

Ti-6Al-4V is highly biocompatible, promoting cellular adhesion, proliferation, and osseointegration, all of which are necessary for good implant fixation and bone-implant interface stability [1]. Furthermore, the alloy's improved fatigue resistance and fracture toughness enable consistent performance under cyclic biomechanical stress conditions observed in vivo. These characteristics collectively make Ti-6Al-4V a standard material for load-bearing biomedical components, including orthopaedic implants, dental fixtures, cardiovascular devices, and minimally invasive surgical instruments [2]. Titanium alloys are intrinsically difficult to machine by traditional techniques due to their low thermal conductivity and elastic modulus, and high chemical reactivity. Attempts to produce Ti alloys using traditional techniques result in mechanical damage, frequent tool wear, high machining costs, and deterioration of work surface quality [3]. Modern machining techniques can overcome such difficulties, including photochemical machining (PCM), which uses controlled chemical etching to produce intricate features and complex geometries in Ti alloys, a difficult-to-machine material [4]. PCM is a low-cost manufacturing technology to fabricate burr- and stress-free parts. and has the potential to fabricate precision components required for biomedical applications [5,6]. PCM enables the simultaneous manufacturing of multiple parts with minimal setup time and equipment requirements, making it ideal for low-volume production and prototyping applications [7].

Despite these benefits, machining Ti alloys with PCM presents unique challenges, including the development of a stable passive oxide layer that limits uniform material dissolution, difficulties in controlling the etch rate, and a tendency toward lateral etching that leads to undercutting and dimensional inaccuracies [8]. Effective control of process parameters and etchant chemistry is therefore essential for obtaining consistent etching behaviour and high

surface quality, thereby facilitating the machining of Ti alloy materials. Some important past attempts by various researchers on PCM of various materials are discussed below.

An examination of chemical etchants for aluminium alloys highlighted the efficiency of ferric chloride ($FeCl_3$), sodium hydroxide (NaOH), and hydrochloric acid (HCl) for shaping Al at relatively moderate etchant temperatures [9]. HCl had the highest etch rate, whereas NaOH provided an improved surface finish. This highlights the trade-off between material removal efficiency and surface quality in chemical machining of Al alloys. A study on PCM machining of steel surfaces produced circular-line (CL) and circular-wavy (CW) surface textures using HNO_3 as an etchant [10]. Tribological testing under lubricated conditions revealed that smaller CL textures condensed friction and increased resistance to wear for untextured surfaces, attributed to better lubricant retention and more effective debris trapping. According to a study on Monel 400 PCM, higher residual stresses caused the etch depth to rise from 42.2 µm to 49.2 µm [11]. Increasing etchant temperature and etching duration increased depth and undercutting. Line sharpness and resist endurance were enhanced by the ideal photoresist exposure of 120s. The effects of etching time, $FeCl_3$ concentration, and the HCl-to-$FeCl_3$ ratio on micro-groove dimensions and geometric correctness were examined in a PCM study of 100Cr6 steel [12]. Prolonged etching increased errors, while higher $FeCl_3$ concentrations reduced them, producing grooves of 3,056 µm length, 625 µm width, 48 µm depth, and surface roughness Ra = 1.285 µm. In another work, during PCM machining of Inconel 601, a maximum material removal rate (MRR) of 0.390 mm^3/min and a minimum undercut (UC) of 0.180 mm were achieved at 47 °C, 800 g/L $FeCl_3$ concentration, and 5 min etching time [13]. Among the process parameters, etching time was shown to be the most influential, underscoring the importance of precise time control in nickel-based superalloy PCM to balance material removal with geometric accuracy. A maximum MRR of 2.95 mg/min at 70 °C and a minimum surface roughness (SR) of 1.27 µm at 40 °C were obtained when PCM was applied to AZ91D magnesium alloy [14]. The analysis determined that the most relevant parameters for MRR and SR were etching concentration and etching temperature (ETE). The PCM of Muntz metal using $FeCl_3$ was investigated, demonstrating that the MRR rose from 0.0120 to 0.0411 g/min and SR from 2.3230 to 17.213 µm when the ETE and etching time (ET) increased [15]. Prolonged etching reduced ED from 1415.2 to 49.3 µm, demonstrating a balance between material removal and edge perfection. PCM on Cu-Zn alloys employing a full factorial design showed that moderate etchant concentrations of 300-400 g/L and a temperature of roughly 45 °C produced balanced performance, producing lower surface roughness and edge deviation with an average MRR of ~0.0015 g/min [16]. Higher concentrations (700 g/L) greatly increased the MRR to ~0.0049 g/min but resulted in lower surface quality due to vigorous etching.

According to a comprehensive literature review, there are surprisingly few systematic parametric investigations of the PCM process for Ti-6Al-4V in biomedical applications. While Ti-6Al-4V has been widely machined using various traditional and non-traditional production techniques, little attention has been given to the PCM process. This work is unique in that it extends the HF-HNO_3 composition window by mixing DI water to balance and control etching parameters for precision micro-feature development on Ti-6Al-4V for biomedical applications. Furthermore, the work emphasizes the need for regulated material removal and surface integrity in micro-scale biomedical components employing the PCM process, which has received less attention in previous studies. The present study investigates the PCM behaviour of Ti-6Al-4V with an emphasis on fabricating square-shaped micro-cavities using a novel chemical etchant. A novel chemical etchant of HF-HNO_3 with different combinations due to its chemical compatibility with Ti-6Al-4V and suitability for biomedical-grade components was employed. Moreover, the goal of this study is to determine how well this etchant performs in terms of controlled material removal, better feature definition, and surface integrity. Furthermore, the dimensional precision, surface quality, and overall process productivity of PCM to produce Ti-6Al-4V biomedical components have been quantitatively evaluated in this work.

2 Materials and Methods

This work investigated the mechanistic significance of a novel HF-HNO_3-based chemical etchant in the PCM process using 1 mm thick Ti-6Al-4V sheets. Ti-6Al-4V is widely used in biomedical applications due to its exceptional biocompatibility, high specific strength, and outstanding corrosion resistance. Chemical

etching is essential for revealing microstructural characteristics, such as grain boundaries, phases, and flaws, in materials. Titanium alloys are difficult to etch, with commonly used etchants including Kroll's reagent (HF + HNO_3 + H_2O), nitric-acid-based solutions, hydrochloric-acid solutions, and electrolytic etching methods [17]. However, these classic etchants have limits in terms of etching uniformity, surface morphology control, and overall process stability. The proposed hybrid HF etchant, which combines HF with other acids or modifiers, has various advantages over traditional single-acid etchants [18]. Compared with traditional single-acid etchants, this novel etchant offers higher etching efficiency, greater surface uniformity, and increased microstructural contrast, making it ideal for Titanium and ferrous alloys. However, creating a dense, adherent TiO_2 passive layer that controls its intrinsic chemical stability poses a serious obstacle to traditional chemical machining [2]. By forming soluble titanium fluoride complexes, HF selectively dissolves the protective TiO_2 layer, and HNO_3 serves as a controlled oxidising agent that regulates metal dissolution and stabilises etching kinetics [19]. This synergistic reaction mechanism enables the proposed HF–HNO_3 etchant system to effectively overcome this limitation by balancing surface activation and oxide dissolution, thereby suppressing localized pitting, improving feature definition during PCM, and ensuring uniform and sustained material removal throughout the etching process.

HF is a highly reactive and toxic chemical; thus, proper safety and environmental precautions were taken during the etching process. HF-based etchants were handled in controlled laboratory facilities utilizing corrosion-resistant containers, proper ventilation systems, and appropriate personal protective equipment to reduce health concerns. Moreover, adequate waste management protocols and environmental standards were followed to prevent contamination and ensure the safe industrial application of the etching process.

To investigate the influence of essential process parameters, namely, etchant composition (vol.%) (EC) and etching time (ET), on reaction kinetics, mass transport behaviour, and etch asymmetry that further influence surface integrity, geometric accuracy, and MRR, systematic experiments were carried out under various operating conditions. The response parameters edge deviation (ED), material removal rate (MRR), and mean roughness depth (Rz) were selected to thoroughly evaluate the performance of the PCM process. ED is an important measure of dimensional precision and undercutting during isotropic chemical dissolution, as it directly impacts the fidelity of microfeature geometry. MRR measures the PCM process's machining efficiency and productivity, which is highly dependent on etchant concentration, temperature, and diffusion kinetics. The mean roughness depth (Rz) was chosen to assess the surface integrity and microtopographical quality of the etched features, which are critical for functional performance and post-processing requirements. Therefore, a balanced evaluation of accuracy, productivity, and surface quality in the PCM process can be carried out by selecting ED, MRR, and Rz.

Table 1 summarizes the experimental matrix and the selected parameter levels. Etchant concentration, temperature, and photoresist properties are some of the process variables that affect PCM machining. Since EC and ET have the greatest impact on material removal kinetics and surface integrity of Ti-6Al-4V, they were selected as the main variable process parameters in this work. To separate the individual and combined impacts of the chosen variables, other factors, including etchant temperature and photoresist thickness, are kept constant throughout the experimentation.

Figure 1 depicts various steps employed during PCM machining of Ti-6Al-4V. The material is initially dressed in acetone to eliminate organic residues and surface impurities, improving photoresist adherence and pattern accuracy. To stabilize the film, a uniform photoresist layer is placed via immersion coating and subsequently dried under regulated conditions. To transfer the pattern, a 5 mm × 5 mm square photomask was aligned over the coated surface and exposed to the vacuum-assisted ultraviolet (UV) for about 120 seconds. This exposure selectively altered the photoresist's solubility in the uncovered portions, defining the etch pattern for machining. Following UV exposure, the specimen was developed in a solvent-based solution that selectively removed unexposed portions of the negative photoresist, revealing the underlying metal.

The sample was then washed to remove any remaining developer and maintain pattern integrity. Chemical etching involved immersing the specimen in a temperature-controlled HF and HNO_3 solution, resulting in the uniform and controlled dissolution of exposed metal areas. The HF-HNO_3 aqueous etchant provides a controlled and reliable mechanism for

dissolving an otherwise very passive metal [20]. Hydrofluoric acid selectively dissolves the stable TiO_2 passive coating, allowing for continuous metal dissolving, while nitric acid functions as an oxidizing and moderating agent, limiting uncontrolled attack and hydrogen evolution. This synergistic effect produces uniform etch rates, enhanced surface quality, and predictable undercut behavior, all of which are important for geometric accuracy in PCM procedures. The presence of HNO_3 minimizes the likelihood of hydrogen embrittlement, particularly in α-β alloys like Ti-6Al-4V [21].

The HF-HNO_3 system is a cost-effective and industrially proven solution for precision titanium machining. It is compatible with common photoresist masks, scalable for immersion or spray etching, and can be adjusted for numerous titanium grades with small compositional changes.

Table 1: Details of parameters used in the present study

Fixed parameters			
Workpiece size	20mm×20mm×1mm		
Desired square shape	5mm×5mm		
Chemical etchant	HF: HNO_3		
Process parameters			
Parameters	**Levels**	**Values**	**Symbolic Notation**
Etchant composition (vol.%)	5	HF: 1.5 %, HNO_3: 15 %, DI Water: Balance	E1
		HF: 2 %, HNO_3: 18 %, DI Water: Balance	E2
		HF: 2.5 %, HNO_3: 21 %, DI Water: Balance	E3
		HF: 3 %, HNO_3: 24 %, DI Water: Balance	E4
		HF: 3.5 %, HNO_3: 27 %, DI Water: Balance	E5
Etching time (sec)	5	20, 30, 40, 50, 60	

Figure 1: Experimental setup employed for PCM machining of Ti-6Al-4V alloy.

Adopting a suitable Design of Experiments (DoE) technique is an essential part of any experimental study to scientifically investigate the subject matter [22]. A full factorial design of experiment (DoE) technique with 25 trial runs (5^2) is used for obtaining possible combinations of process parameters, etchant composition and etching time to carry out experiments/tests to evaluate their effects on edge deviation (ED), material removal rate (MRR), and mean roughness depth (Rz). The selection of parameters and their levels was based on preliminary trials and relevant literature. The experiments' statistical design and analysis were carried out using Minitab 17 software, which was used to generate the experimental layout, conduct Analysis of Variance (ANOVA), and assess the impact of process parameters on response characteristics. This structured DoE approach enabled a thorough evaluation of the relationships between process parameters and indicators for geometric accuracy, material removal rate, and surface quality.

A Leica DM 2500M optical microscope was used to measure edge deviation after each machining trial. Mean roughness depth of the machined specimens was then assessed using a Handysurf E-35B surface profilometer (Tokyo Seimitsu Co. Ltd.). The MRR for each experimental run was calculated using Eq. (1), which accounts for the recorded machining time and the change in specimen mass before and after machining.

$$MRR = \frac{(Wi-Wf)}{T} \quad (1)$$

Where T is the machining time, Wi is the workpiece's initial weight, and Wf is its final weight.

Analysis of Variance (ANOVA) was used to determine the statistical significance and level of contribution of process parameters affecting the responses. Further, an optimization framework, the Overall Evaluation Criterion (OEC), was implemented to determine optimal PCM process settings for MRR, ED, and Rz. OEC necessitated the assignment of relevant quality characteristics (QC) in order to turn various objectives into a single performance index, considering the conflicting nature of responses. To prioritize geometric accuracy and surface integrity, ED and Rz were considered as "lower-is-better" quality characteristics (QC = S), as reductions in these responses immediately enhance geometric precision, reduce edge distortion, and improve surface smoothness of Ti-6Al-4V components. In contrast, process productivity in terms of MRR was assigned "higher-is-better" quality characteristic (QC = L), indicating the requirement to maximize etching efficiency and throughput during the PCM process. This differential QC allows the OEC technique to balance quality and productivity goals within a single optimization framework. The aggregated performance score for each experimental setting was calculated by assessing the OEC using Eq. (2), which allowed optimal parameter combinations to be identified based on overall process efficacy.

$$OEC = \left(\left(\frac{P-P_{min}}{P_{max}-P_{min}}\right) \times W_P\right) + \left(\left(1 - \left(\frac{Q-Q_{min}}{Q_{max}-Q_{min}}\right) \times W_Q\right)\right) + \left(\left(1\left(\frac{R-R_{min}}{R_{max}-R_{min}}\right) \times W_R\right)\right) \quad (2)$$

Where W_P, W_Q, and W_R are weight percentages assigned to P, Q, and R, respectively; MRR, ED, and Rz are represented by P, Q, and R, respectively.

As a result, the purposeful choice of the "higher-is-better" quality characteristic (QC = L) for MRR and the "lower-is-better" quality characteristic (QC = S) for ED and Rz allowed the OEC technique to systematically balance productivity-driven and quality-driven objectives. This balanced formulation made it easier to identify the best combination of PCM process parameters for machining Ti-6Al-4V, resulting in improved material removal efficiency while maintaining controlled edge accuracy and surface integrity.

3 Results and Discussion

Table 2 presents the full matrix of variable input parameters' combinations and corresponding values of responses. The measured MRR ranges from 0.351 to 0.967 mg/min, etch deviation from 29 µm to 54 µm, and Rz from 1.82 µm to 6.13 µm, indicating the substantial relationship between chemical dissolution kinetics and process parameters. Overall, these findings highlight the intrinsic trade-off in Ti-6Al-4V PCM between increased material removal efficiency and preservation of surface quality and dimensional precision.

Figures 2 (a-b) present optical microscope images of the machined feature obtained at experimental conditions 1 and 25, respectively, demonstrating the achieved geometric integrity and dimensional precision of the fabricated structure.

Table 2: Combinations of process parameters and corresponding experimental results during PCM of Ti-6Al-4V

Ex. No	Process parameters		Response measures			
	Etchant Composition (vol.%)	Etching time (sec)	Edge deviation (µm)	MRR (mg/min)	Rz (µm)	OEC
1	E1	20	34	0.351	1.82	60.00
2	E1	30	32	0.496	2.19	67.72
3	E1	40	29	0.524	2.22	73.01
4	E1	50	31	0.652	2.31	76.57
5	E1	60	32	0.405	2.48	60.55
6	E2	20	42	0.547	2.53	54.51
7	E2	30	40	0.638	3.02	58.31
8	E2	40	37	0.653	2.73	65.37
9	E2	50	39	0.679	2.69	64.42
10	E2	60	34	0.541	2.82	62.61
11	E3	20	43	0.654	3.07	54.78
12	E3	30	41	0.735	2.95	62.76
13	E3	40	45	0.757	2.77	60.01
14	E3	50	40	0.781	2.89	67.05
15	E3	60	37	0.696	2.63	68.47
16	E4	20	51	0.695	3.42	43.62
17	E4	30	53	0.818	3.62	46.06
18	E4	40	47	0.926	3.58	60.21
19	E4	50	50	0.942	3.82	55.22
20	E4	60	42	0.967	4.02	65.69
21	E5	20	54	0.793	4.19	38.95
22	E5	30	48	0.872	4.57	48.28
23	E5	40	51	0.903	5.14	41.54
24	E5	50	45	0.935	6.13	43.60
25	E5	60	48	0.764	5.95	31.74

Figures 3(a-b) present the precise morphologies of the etched edges that form the full square cavity at experimental conditions 1 and 25. The regularity of the edge profiles and well-defined cavity boundaries observed under both conditions validate the PCM process's resilience and repeatability, demonstrating its ability to generate precision micro-components from Ti-6Al-4V with high dimensional fidelity for biomedical applications.

3.1 *XRD and SEM analysis*

The SEM and XRD investigations provide insight into the underlying mechanism that controls the observed etching behaviour and surface properties. The XRD patterns of raw and PCM-machined Ti-6Al-4V samples, depicted in Fig. 4, exhibit diffraction peaks at around 35.1°, 38.4°, 40.2°, 53.0°, and 63.0°, which correspond to the (100), (002), (101), (102), and (110) planes of the α-Ti (HCP) phase. Both samples have identical peak positions, indicating that photochemical machining has no effect on the bulk crystalline structure or induces a phase transition. Minor differences in peak intensities and peak broadening seen in the PCM-treated sample can be attributed to near-surface factors such as residual stresses, microstrain, and chemical etching-induced localised lattice deformation. The diffraction peak positions in the XRD patterns of raw and PCM-machined Ti-6Al-4V are similar, indicating that photochemical machining preserves the alloy's bulk crystallographic structure.

The dual-phase character of Ti-6Al-4V is supported by the diffraction profiles, which are dominated by α-Ti (HCP) phase reflections with small β-Ti contributions. There is no indication of phase transformation or secondary phase formation, and the little fluctuations in peak intensity and marginal peak broadening seen during PCM are attributable to near-surface factors such as residual stresses, microstrain, and localised lattice distortions caused by chemical etching. The XRD results provide evidence for this mechanism by showing changes in the intensities of some crystalline peaks after etching, suggesting partial dissolution or phase alteration.

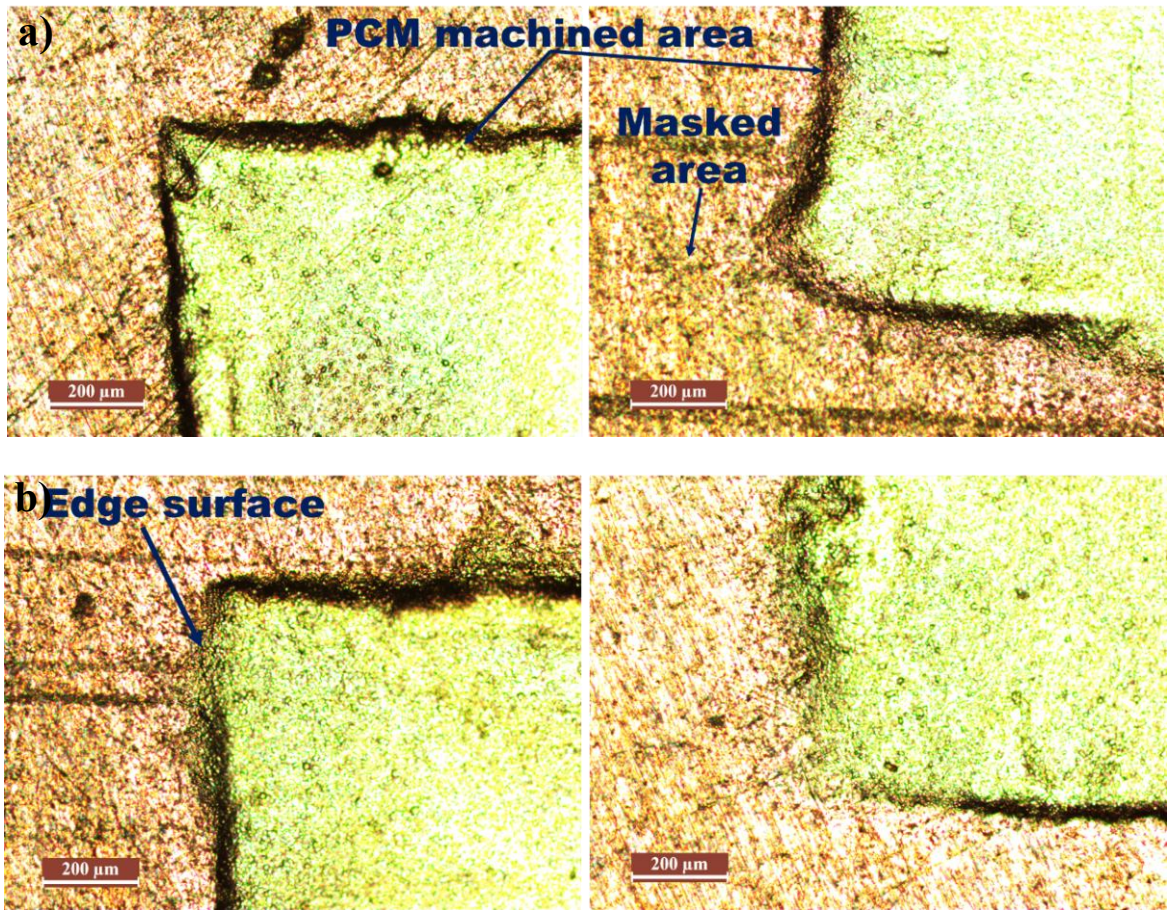

Figure 2: Optical micrographs showing the edge surface of the square cavity machined at different experimental conditions. (a) Machining condition 1. (b) Machining condition 25.

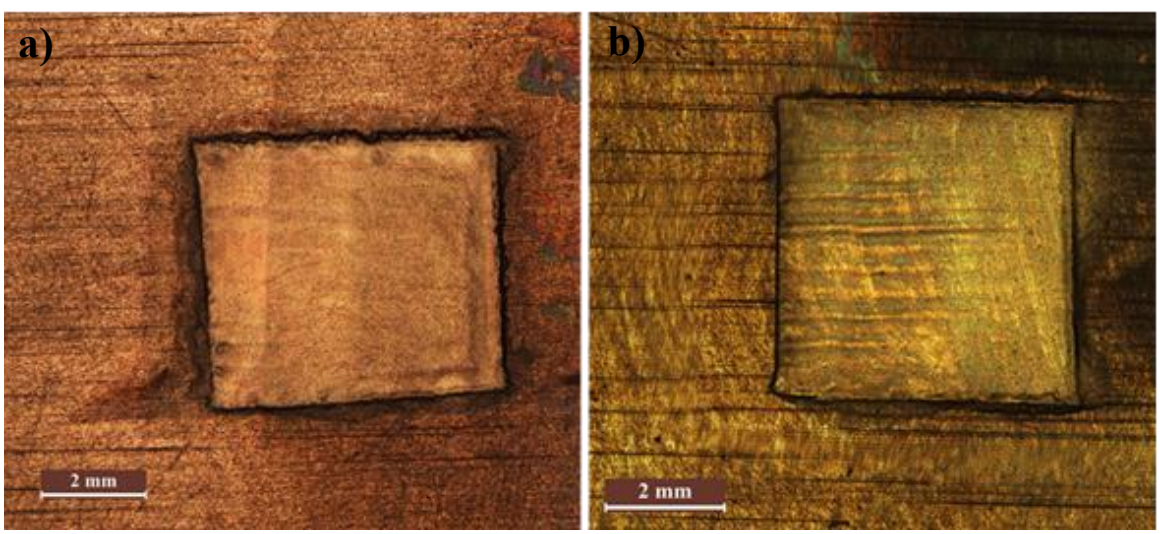

Figure 3: Optical micrographs of the entire square cavity structure formed on Ti-6Al-4V at different experimental conditions. (a) Experimental run 1. (b) Experimental run 25.

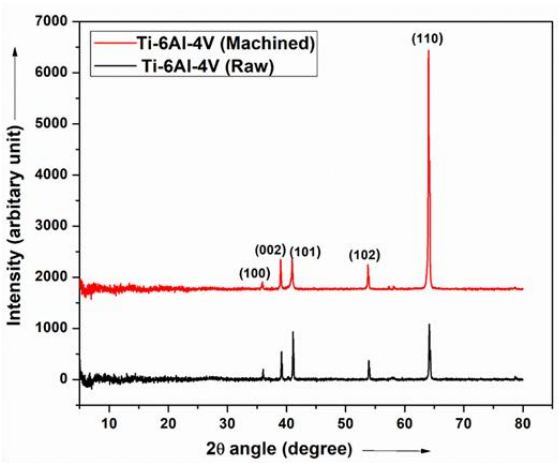

Figure 4: XRD examination of unmachined and PCM-machined Ti-6Al-4V samples.

SEM study of Ti-6Al-4V surfaces produced by PCM machining reveals distinctive corrosion characteristics arising from the alloy's dual-phase microstructure, as depicted in Figure 5. Preferential phase corrosion is observed, with the β-phase (vanadium-rich) exhibiting relative resistance and the α-phase experiencing localized anodic dissolution, resulting in shallow etch depressions at phase boundaries. Micro-galvanic corrosion is observed, with increased material loss around α/β contacts due to electrochemical potential changes [23]. Under optimal PCM circumstances, the etching appeared uniform, giving smooth surface texturing with negligible roughness. However, higher etchant concentrations or longer exposure led to small, localized pitting and slight edge undercutting behind the photoresist mask. Overall, SEM observations demonstrate that PCM induces regulated, phase-dependent chemical dissolution, enabling high-fidelity production of Ti-6Al-4V features with minimal microstructural damage. Chemical etching produces microgalvanic cells in the Ti-6Al-4V alloy, where lower electrochemical-potential phases act as anodic areas and dissolve preferentially in the HF-HNO_3 etchant. This selective phase dissolution promoted localised material removal, resulting in micro-pits and uneven surface characteristics as seen in SEM micrographs. Under favourable etching conditions, the increased dissolution rate resulted in higher ED and MRR. At the same time, the gradual formation of micro-pits and an uneven surface morphology resulted in higher Rz.

The combined results of XRD and SEM investigations reveal that PCM machining of Ti-6Al-4V primarily affects the surface microstructure without altering the bulk phase composition. SEM images show the formation of micro-voids and micro-galvanic corrosion, indicating controlled electrochemical dissolution along specified microstructural paths. Concurrently, XRD patterns reveal that the α-Ti (HCP) phase is retained, with modest β-Ti contributions, demonstrating that the PCM process selectively alters the surface while retaining the material's intrinsic metallurgical integrity [24]. These findings emphasize PCM as a precise, non-destructive surface engineering technology capable of removing targeted material while preserving the structural integrity of the titanium alloy.

3.2 *Effects of Process Parameters*

Edge deviation (ED) is employed to assess dimensional correctness in PCM-fabricated samples. It is defined as the greatest perpendicular distance between the nominal and measured edge profiles. ED for vertical and horizontal edges is calculated as the absolute difference between nominal and measured coordinates. The reported ED for each specimen is the highest divergence between all evaluated edges. Because of the isotropic material breakdown in PCM, edge rounding and lateral undercutting beneath the photoresist are inescapable, with ED generally scaling with etch depth and serving as a measure of geometric accuracy. As illustrated in Figure 6, ED increases monotonically with etchant concentration, owing to faster reaction rates and increased lateral material removal at feature boundaries [25]. In contrast, as etching time increases, ED reduces because extended exposure promotes homogeneous disintegration and progressive attenuation of local geometric imperfections, resulting in a lower maximum deviation [26]. Furthermore, a decrease in ED during longer etching durations is associated with the generation of reaction products and surface passivation, which reduces the effective dissolution rate. Using the HF-HNO_3 etchant on Ti-6Al-4V alloy, which has inherent corrosion resistance, promotes the formation of a partially protective surface layer after prolonged exposure, preventing further material dissolution.

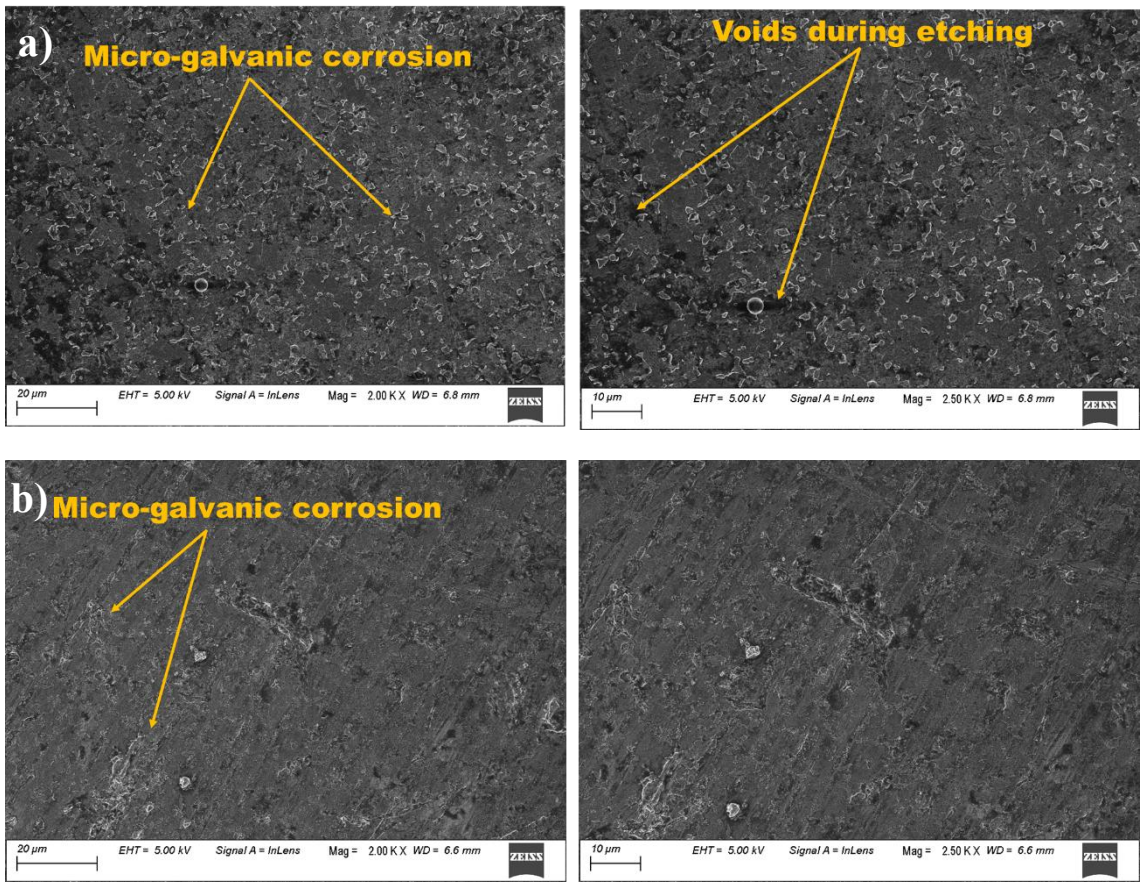

Figure 5: SEM analysis of the PCM machined surface at various experimental conditions. (a) Machining condition 1. (b) Machining condition 25.

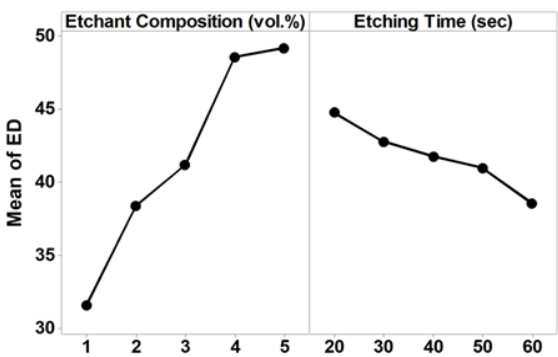

Figure 6: Influence of etchant composition and etching time on edge deviation in PCM of Ti-6Al-4V.

The minimum ED of 29 µm is achieved at an etchant composition of (HF: 1.5 %, HNO_3: 15 %, DI Water: Balance), and an etching duration of 40 s. These results indicate that lower chemical intensities favour improved geometric accuracy in photochemical machining, highlighting the importance of carefully controlling process parameters to achieve precise material removal.

Interaction plots were generated to investigate the combined effect of process parameters on response variables. The potential interaction effects between etchant composition and etching time on photochemical machining responses were analyzed. Figure 7 shows the interaction plot of the combined effect of EC and ET on ED. Higher HF-HNO_3 ratios lead to greater chemical reactivity, resulting in a higher ED. With increasing ET, ED initially rises and then gradually stabilises at longer durations, potentially due to over-etching effects or partial surface passivation. The non-parallel, crossing

interaction lines indicate a moderate interaction between the process parameters, suggesting that ET's influence depends on EC. From composition levels 1 to 4, ED grows significantly, then stabilises or slightly declines. Longer etching times (50-60 s) generally yield higher ED values than shorter intervals, indicating greater lateral material disintegration. Overall, a lower etchant composition and shorter etching time yield the lowest ED, whereas a higher composition and longer exposure time yield the highest geometrical deviation. The interaction plot for ED shows that both EC and ET significantly influence the geometric accuracy of the etched features.

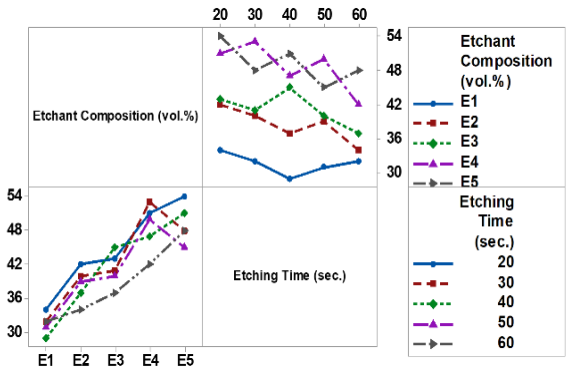

Figure 7: Interaction plot of EC and ET on ED in PCM of Ti-6Al-4V.

Material removal in PCM machining of Ti-6Al-4V is controlled by chemical dissolution of selectively exposed portions following photoresist patterning. The MRR is principally determined by etchant content, temperature, and exposure duration. Higher etchant concentrations improve reaction kinetics by increasing the availability of reactive species, thereby enhancing MRR, whereas effective agitation enhances uniform etching by improving mass transfer. Figure 8 shows that MRR increases proportionally with etchant concentration [27]. However, the effect of etching time is nonlinear; MRR first increases, then decreases, due to depletion of active species and the buildup of reaction by-products, which lower reaction efficiency. The highest MRR of 0.967 mg/min is obtained at an etchant composition of (HF: 3 %, HNO_3: 24 %, DI Water: Balance) and an etching duration of 60 s, indicating that higher chemical intensities and etching duration enhance reaction kinetics in photochemical machining.

The interaction plot in Figure. 9 shows that MRR rises dramatically with increasing EC and ET, indicating their major influence on the chemical dissolution rate during photochemical machining. MRR consistently rises with ET across all compositions, with higher EC levels (E4-E5) producing the most material removal due to increased chemical reactivity. A significant rise in MRR is found from composition level E1 to E4, indicating the importance of EC in boosting machine productivity. However, a modest decrease in MRR at the highest EC level and prolonged ET suggests surface saturation, reaction product accumulation, or diffusion-controlled etching. The non-parallel interaction lines suggest that the parameters interact to some extent, implying that the influence of ET depends on the EC used. Overall, a higher EC and longer ET result in the maximum MRR, whereas lower levels limit machining efficiency.

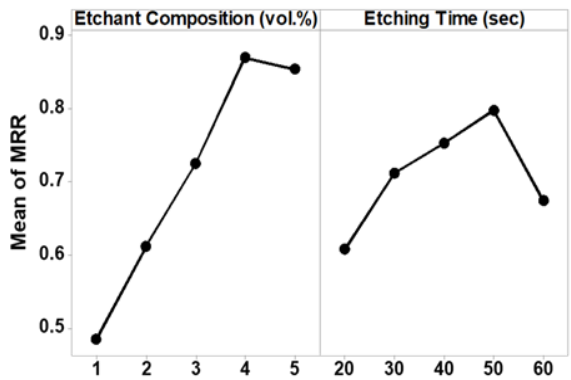

Figure 8: Influence of etchant composition and etching time on MRR in PCM of Ti-6Al-4V.

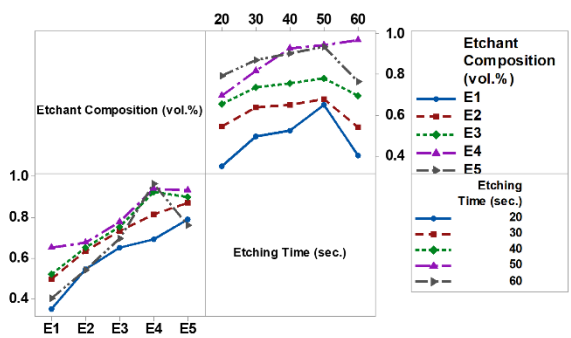

Figure 9: Interaction plot of EC and ET on MRR in PCM of Ti-6Al-4V.

In this study, the surface roughness (SR) parameter, mean roughness depth (Rz), is used to quantitatively assess the surface quality of PCM-machined samples. On five equal sections along the

evaluation length, Rz measures the average value of the highest peaks to the deepest valleys. Rz detects acute asperities important to determine the performance of surfaces from tissue injury, increased wear, and bacterial adhesion points of view in biomedical applications.

Figure 10 depicts the impact of process parameters on Rz. An increase in the etchant composition (vol.%) results in higher SR due to increased chemical activity, leading to non-uniform material dissolution and decreased surface quality [28]. Similarly, increased etching time increases Rz because continual reactions and lateral etching result in excessive material loss. The near-linear trend in SR is related to the interaction between etchant composition and concentration. The smallest SR of Rz 1.82 µm is achieved with an etchant composition of (HF: 1.5 %, HNO_3: 15 %, DI Water: Balance) and an etching duration of 20 s, demonstrating that lower chemical intensities and shorter etching duration enhance surface integrity in photochemical machining.

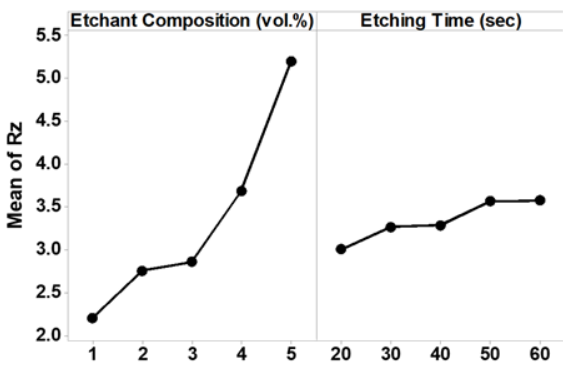

Figure 10: Influence of etchant composition and etching time on mean roughness depth in PCM of Ti-6Al-4V.

Rz rises as EC and ET increase, as indicated by the interaction plot in Figure 11, suggesting increasing chemical attack and irregular material dissolution during photochemical machining. Due to aggressive etching kinetics and potential micro-pitting effects, higher composition levels (E4-E5) routinely produce higher Rz values, especially at longer ET. The non-parallel interaction lines indicate a moderate interaction between EC and ET, meaning that the effect of exposure time varies with chemical concentration. Overall, lower EC and shorter ET result in a better surface finish, whereas higher EC and longer ET increase surface roughness.

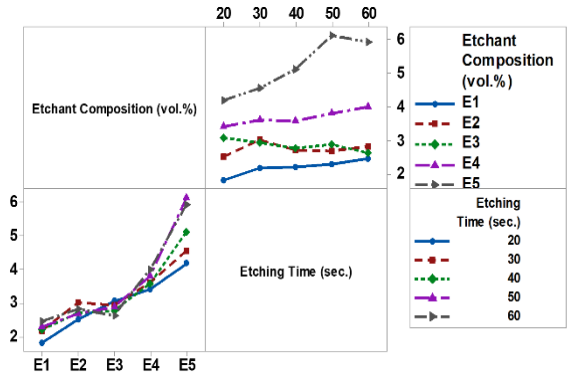

Figure 11: Interaction plot of EC and ET on mean roughness depth in PCM of Ti-6Al-4V.

3.3 *ANOVA and OEC*

Using Minitab statistical analysis software, regression models were developed to predict ED, MRR and Rz as functions of EC and ET. These models helped develop a quantitative relationship between process parameters and machining performance, enabling the prediction of response values for various EC and ET combinations. The regression equations for ED, MRR and Rz are presented in equations (3), (4) and (5), respectively. The coefficients in the equations represent each factor level's relative contribution to the corresponding response, providing insight into the way EC and ET affect surface quality, material removal behaviour, and ED during photochemical machining.

$$ED = 41.80 - 10.20 \times EC\_1 - 3.40 \times EC\_2 - 0.60 \times EC\_3 + 6.80 \times EC\_4 + 7.40 \times EC\_5 + 3.00 \times ET\_20 + 1.00 \times ET\_30 - 0.00 \times ET\_40 - 0.80 \times ET\_50 - 3.20 \times ET\_60 \quad (3)$$

$$MRR = 0.7090 - 0.2234 \times EC\_1 - 0.0974 \times EC\_2 + 0.0156 \times EC\_3 + 0.1606 \times EC\_4 + 0.1444 \times EC\_5 - 0.1010 \times ET\_20 + 0.0028 \times ET\_30 + 0.0436 \times ET\_40 + 0.0888 \times ET\_50 - 0.0344 \times ET\_60 \quad (4)$$

$$Rz = 3.3428 - 1.137 \times EC\_1 - 0.585 \times EC\_2 - 0.481 \times EC\_3 + 0.349 \times EC\_4 + 1.853 \times EC\_5 - 0.335 \times ET\_20 - 0.073 \times ET\_30 - 0.055ET\_40 + 0.225 \times ET\_50 + 0.237ET\_60 \quad (5)$$

The effects of process parameters on response variables were systematically assessed at the 95% confidence level using ANOVA. In this study, the statistical significance of each process parameter was determined using the probability value (p-value)

obtained from the ANOVA findings [29]. The parameter is statistically significant if the *p*-value is ≤ 0.05, indicating a meaningful influence on the response variable. Table 3 presents the complete ANOVA results for edge deviation (ED), material removal rate (MRR), and mean roughness depth (Rz). The results show that the influence of the process parameters changes based on the response characteristic under consideration. Among the examined characteristics, etchant composition was discovered to be the most important parameter influencing all three responses. Specifically, the etchant composition accounted for 83.96% of the total variance in ED, 77.12% in MRR, and 88.46% in Rz, highlighting its crucial role in managing geometric precision, machining efficiency, and surface integrity during PCM. The high contribution % indicates that the etchant's chemical reactivity and concentration significantly impact material dissolution and surface shape.

The adequacy and predictive capability of the developed statistical models were evaluated using the coefficient of determination (R^2) and the adjusted coefficient of determination (R^2(adj). The R^2 value is the proportion of the total variability in the response that the regression model explains. R^2(adj) is a more reliable measure of model fitness since it accounts for the number of predictors in the model. The R^2 values of 92.04% for ED, 93.21% for MRR, and 92.17% for Rz demonstrate a positive correlation between experimental and projected results, potentially validating the effectiveness of the models and equations. Overall, the ANOVA findings demonstrate that the suggested statistical models are statistically significant and capable of accurately predicting response behavior, as well as revealing the predominant role of etchant composition on PCM process performance.

A multi-objective optimization framework is required to determine the optimal set of process parameters, as it accounts for all relevant response measures simultaneously rather than optimizing each response individually.

Table 3: Analysis of Variance for edge deviation, MRR, and mean roughness depth.

Edge Deviation					
Source	**Adj SS**	**Adj MS**	**F**	**P**	**% contribution**
Etchant Composition (vol.%)	1084.8	271.200	42.21	0.000	83.96
Etching Time (sec)	104.4	26.100	4.06	0.018	8.08
Residual error	102.8	6.425			7.96
R^2=92.04%, R^2 (adj) = 88.07%					
Material Removal Rate					
Etchant Composition (vol.%)	0.53141	0.132852	45.80	0.000	77.12
Etching Time (sec)	0.10589	0.026473	9.13	0.000	15.49
Residual error	0.04641	0.002900			6.79
R^2=93.21%, R^2 (adj) = 89.82%					
Surface roughness					
Etchant Composition (vol.%)	27.109	6.7772	45.21	0.000	88.46
Etching Time (sec)	1.137	0.2842	1.90	0.160	3.71
Residual error	2.398	0.1499			7.83
R^2=92.17%, R^2 (adj) = 88.26%					

Applied Science and Engineering Progress, Vol. 20, No. 2, 2027, 8192

Table 4: Process conditions used to evaluate the OEC.

Response	Worst	Best	Quality characteristics	Weight
ED (μm)	54	29	S	33.34
MRR (mg/min)	0.351	0.967	L	33.33
Rz (μm)	6.13	1.82	S	33.33

In the current study, the OEC approach is used as a single aggregated performance indicator, allowing for multi-objective optimisation across the selected responses.The OEC technique converts responses with different scales and units into a dimensionless, normalised index, enabling full comparison across experimental settings. In the OEC computation, the responses were assigned approximately equal weights: 33.34% to ED and 33.33% to MRR and Rz, indicating their comparable significance in evaluating overall machining performance. ED denotes the geometric accuracy of the etched feature, MRR measures process productivity, and Rz describes the machined surface's surface integrity. Because all three responses influence the efficacy of the photochemical machining process, equal weighting was used to eliminate bias toward any particular performance measure. This balanced weighting approach allows for a comprehensive evaluation of the process by accounting for etching precision, machining efficiency, and surface quality simultaneously. Table 4 shows the weights allocated to each response, as well as the best and worst values utilized in the normalization technique. Table 4 summarizes the determined OEC values for each experimental run, which correspond to different combinations of process parameters, and serves as the foundation for determining the ideal machining conditions.

The greatest OEC value of 76.57 is attained through an etchant composition of (HF: 2 %, HNO_3: 15 %, DI Water: Balance) and an etching duration of 50 s. This precise set of process settings represents the best compromise among the performance characteristics, resulting in a better balance between material removal efficiency and surface quality. As a result, the parameter set associated with experimental condition 4 is recognized as the ideal operating state for simultaneous multi-response optimization of ED, MRR, and Rz. The increased OEC value under these conditions confirms the efficiency of this parameter combination in increasing machining productivity while maintaining geometric accuracy and surface integrity during photochemical machining of Ti-6Al-4V.

4 Conclusions

In this research, PCM has successfully fabricated a square cavity in a Ti-6Al-4V workpiece. The novel HF-HNO_3 chemical etchant proved effective for producing biomedical components from PCM. Based on the findings of this study, the following conclusions can be drawn:

- The lowest ED (29 μm) was achieved with a low-intensity etchant (1.5% HF, 15% HNO_3) for 40 seconds, resulting in minimal lateral undercutting.
- The maximum MRR (0.967 mg/min) was achieved with 3% HF and 24% HNO_3 at 60 s. Higher chemical intensity and longer etching time improved reaction kinetics and PCM productivity.
- Using a low-intensity etchant (1.5% HF and 15% HNO_3) at 20 s resulted in the lowest mean roughness depth (Rz = 1.82 μm), indicating better surface integrity during PCM.
- ANOVA demonstrated that EC was the most important parameter, strongly impacting responses in photochemical machining.
- The optimum multi-response performance (OEC = 76.57) was attained using an EC of 1.5% HF and 15% HNO_3 at 50 s ET, corresponding to experimental condition 4.
- This work demonstrated that using a customised HF-HNO_3 etchant enables controlled material removal, high geometric precision, and minimal surface roughness during photochemical machining of Ti-6Al-4V. The process has great potential for biomedical applications, such as microsurgical equipment like micro-forceps, micro-scissors, and micro-needle holders, which require high precision and surface quality.

Future investigations include carrying out additional surface characterisation, such as comparisons with other relevant surface roughness parameters and tests for wettability, corrosion resistance, or cytocompatibility; evaluating surface chemistry, fluoride ion retention, and biocompatibility; and applying machine learning and

sustainable process strategies to further optimise PCM for industrial biomedical applications.

Acknowledgments

The authors sincerely thankful to the Mechanical & Industrial Engineering Technology Department of the University of Johannesburg, as well as Advanced Manufacturing Laboratory in the Department of Mechanical Engineering at National Institute of Technology Silchar (India), for providing the necessary resources for experiments, testing, and measurements.

Author Contributions

P.S.: conceptualization, investigation, data curation, data analysis, writing original draft; K.G.: research design, methodology, data analysis, reviewing and editing; P.K.P.: research design, methodology, data analysis, reviewing and editing. All authors have read and agreed to the published version of the manuscript.

Conflicts of Interest

The authors declare no conflict of interest.

Declaration of generative AI and AI-assisted technologies in the writing process

The authors have not utilised any generative AI tool for any assistance in the writing process.

References

[1] S. Ramakrishnan, "Investigating the effects of abrasive water jet machining parameters on surface integrity and chemical state in machining of Ti-6Al-4V," *Materials Today Communications*, vol. 31, p. 103480, 2022, doi: 10.1016/j.mtcomm.2022.103480.

[2] C. Zhang, D. Zou, M. Mazur, J. P. T. Mo, G. Li, and S. Ding, "The state of the art in machining additively manufactured titanium alloy Ti-6Al-4V," *Materials*, vol. 16, p. 2583, 2023, doi: 10.3390/ma16072583.

[3] A. Pramanik and G. Littlefair, "Machining of titanium alloy (Ti-6Al-4V)—theory to application," *Machining Science and Technology*, vol. 19, no. 1, pp. 1–49, 2015, doi: 10.1080/10910344.2014.991031.

[4] D. Agrawal and D. Kamble, "Optimization of photochemical machining process parameters for manufacturing microfluidic channel," *Materials and Manufacturing Processes*, vol. 34, no. 1, pp. 1–7, 2019, doi: 10.1080/10426914.2018.151 2115.

[5] P. V. Babu, S. Ismail, and B. S. Ben, "Experimental and numerical studies of positive texture effect on friction reduction of sliding contact under mixed lubrication," *Proceedings of the Institution of Mechanical Engineers, Part J: Journal of Engineering Tribology*, vol. 235, no. 2, pp. 360–375, 2021, doi: 10.1177/1350650120930911.

[6] R. M. Mazarbhuiya and M. Rahang, "PCM-assisted reverse electro discharge machining process for pattern generation," *Materials and Manufacturing Processes*, vol. 37, no. 9, pp. 995–1002,2022, doi: 10.1080/10426914.2021. 200 1500.

[7] D. Patil, S. Thorat and M. Sadaiah, "Study of the effect of PCM process parameters on geometry type, Ra, depth of etch, undercut comparing $FeCl_3$ and $CuCl_2$ etchants on Monel 400," *Advanced Materials and Processing Technologies*, vol. 10, no. 3, pp. 1956–1976, 2024, doi: 10.1080/2374068X.2023.2205668.

[8] T. Tiwari, A. Dvivedi, and P. Kumar, "Investigations on the fabrication of a patterned tool by chemical etching," *Materials and Manufacturing Processes*, vol. 36, no. 16, pp. 1840–1852,2021, doi: 10.1080/10426914.2021. d1926491.

[9] O. Çakır, "Etchants for chemical machining of aluminium and its alloys," Acta Physica Polonica A, vol. 135, no. 4, pp. 586–587, 2019, doi: 10.12693/aphyspola.135.586.

[10] A. Basir, S. Liza, K. Fukuda, and N. A. Mat Tahir, "Tribological behaviour of multi-shape photochemical textured surfaces," *Surface Topography: Metrology and Properties*, vol. 11, no. 2, p. 025009, 2023, doi :10.1088/2051-672X/acd0c6.

[11] D. H. Patil and S. Mudigonda, "Effect of rolling direction, temperature, and etching time on photochemical machining of Monel 400 microchannels," *Advances in Materials Science and Engineering*, vol. 2016, p. 6751305, 2016. doi: 10.1155/2016/6751305.

[12] F. N. Samani and E. R. Esfahani, "Experimental study of parameters in micro-photochemical machining using maskless digital projection on

flat surfaces of 100Cr6 steel," *Journal of Micromanufacturing*, 2025, doi: 10.1177/251 d65984241306.

[13] N. D. Misal and M. Sadaiah, "Multi-objective optimization of photochemical machining of Inconel 601 using grey relational analysis," *Materials Today: Proceedings*, vol. 5, no. 2, pp. 5591–5600, 2018, doi: 10.1016/j.matpr.2017.12. 150.

[14] P. Sarmah, E. Tripathi, and P. K. Patowari, "Machinability study of AZ91D alloy using photochemical machining for selective material removal," *Materials Today: Proceedings*, vol. 72, no. 4, pp. 2275–2280, 2023, doi: 10.1016/j.matpr.2022.09.216.

[15] H. Borate and A. Utpat, "Effect of process parameters for photochemical machining of Munz metal," *AIP Conference Proceedings*, vol. 2716, p. 020006, 2023, doi: 10.1063/5.0137363.

[16] H. Borate, A. Utpat, and S. S. Wangikar, "Optimization of photochemical machining parameters for Cu–Zn alloys: A multi-response approach using ANOVA and overall evaluation criteria," *Materials and Manufacturing Processes*, vol. 41, no. 1, pp. 117–135, 2026, doi: 10.1080/10426914.2025.2586503

[17] M. A. Surmeneva et al., "The influence of chemical etching on porous structure and mechanical properties of the Ti-6Al-4V functionally graded porous scaffolds fabricated by EBM," *Materials Chemistry and Physics*, vol. 275, p. 125217, Jan. 2022, doi: 10.1016/j.match emphys.2021.125217.

[18] M. A. Rocha et al., "Effect of double-acid etching (HNO_3/HCl) temperature on the surface and electrochemical properties of $Ti_xNb_\gamma Sn$ alloys (x = 35, 45% and y = 0, 2.5, 5.0, 7.5%) for biomedical applications," *Journal of Materials Engineering and Performance*, pp. 1–7, 2025, doi: 10.1007/s11665-025-11915-x.

[19] H. Lee et al., "Effect of HF/HNO_3 treatment on porous structure and cell penetrability of titanium scaffold," *Materials & Design*, vol. 145, pp. 65–73, 2018, doi: 10.1016/j.matdes.2018.02. 059.

[20] X. Song, X. Wang, S. Wang, S. Liu, and S. Ge, "Experimental study on ultra-precision polishing of Ti-6Al-4V by ultraviolet-induced nanoparticle colloid jet machining," *Materials*, vol. 14, p. 5014, 2021, doi: 10.3390/ma14175014.

[21] Q. Yao et al., "Composition and bioactivity of calcium phosphate coatings on anodic oxide nanotubes formed on pure Ti and Ti-6Al-4V alloy substrates," *Materials Science and Engineering C*, vol. 110, p. 110687, 2020, doi: 10.1016/j.msec.2020.110687.

[22] M. Sriariyanun, et al., "An integrated biorefinery of wood apple kernel for bio-oil and bio-diesel production: Optimization of engine attributes using Taguchi, RSM, and CRITIC–COCOSO hybrid techniques," International Journal of Environmental Research, vol. 19, no. 3, p. 67, 2025, doi: 10.1007/s41742-024-00732-0.

[23] T. P. Sarao, H. Singh, and H. Singh, "Enhancing biocompatibility and corrosion resistance of Ti-6Al-4V alloy by surface modification," *Journal of Thermal Spray Technology*, vol. 27, no. 8, pp. 1388–1400, 2018, doi: 10.1007/s11666-018-0746-7.

[24] W. Q. Chen, S. M. Zhang, and J. Qiu, "Surface analysis and corrosion behavior of pure titanium under fluoride exposure," *The Journal of Prosthetic Dentistry*, vol. 124, no. 2, pp. 239.e1–239.e7, 2020, doi: 10.1016/j.prosdent.2020.02. 022.

[25] A. R. Saraf, M. Sadaiah, "Magnetic field-assisted photochemical machining (MFAPCM) of SS316L," Materials and Manufacturing Processes. Vol. 32, no. 3, pp. 327-332, 2016, doi: 10.1080/10426914.2016.1198014.

[26] Y. Sun, et al., "Quantitative study of oxidation mechanism in photoelectrochemical mechanical polishing," *International Journal of Machine Tools and Manufacture*, vol. 210, p. 104307, 2025, doi: 10.1016/j.ijmachtools2025.104307.

[27] G. Sapkota, R. K. Ghadai, R. Čep, G. Shanmugasundar, J. S. Chohan, and K. Kalita, "Enhancing efficiency in photochemical machining: A multivariate decision-making approach," *Frontiers in Mechanical Engineering*, vol. 10, p. 1325018, 2024, doi: 10.3389/fmech.2024.1325018.

[28] A. A. Pawar, N. D. Misal, A. D. Sapkal, R. H. More, and B. A. Kamble, "Experimental evaluation of etching depth for different steels using photochemical machining," *International Journal of New Technology and Research*, vol. 7, no. 7, pp. 82–88, 2021, doi: 10.31871/IJNTR.7.7.20.

[29] R. H. Myers, D. C. Montgomery, C. M. Anderson-Cook, "Response surface methodology: process and product optimization using designed experiments," *John Wiley & Sons*; 2016.